NeuroImage xxx (2018) 1–13

Contents lists available at ScienceDirect

NeuroImage

journal homepage: www.elsevier.com/locate/neuroimage

The age-dependent relationship between resting heart rate variability and functional brain connectivity

D. Kumral [a,b,*], H.L. Schaare [a,c], F. Beyer [a,d], J. Reinelt [a], M. Uhlig [a,c], F. Liem [a], L. Lampe [a], A. Babayan [a], A. Reiter [e,a], M. Erbey [b], J. Roebbig [a], M. Loeffler [f], M.L. Schroeter [a,f,g], D. Husser [h], A.V. Witte [a], A. Villringer [a,b,d,f,i], M. Gaebler [a,b,f]

[a] Department of Neurology, Max Planck Institute for Human Cognitive and Brain Sciences, Leipzig, Germany
[b] MindBrainBody Institute at the Berlin School of Mind and Brain, Humboldt-Universitaet zu Berlin, Berlin, Germany
[c] International Max Planck Research School NeuroCom, Leipzig, Germany
[d] Subproject A1, Collaborative Research Centre 1052 "Obesity Mechanisms", University of Leipzig, Leipzig, Germany
[e] Lifespan Developmental Neuroscience, Technical University of Dresden, Dresden, Germany
[f] LIFE – Leipzig Research Center for Civilization Diseases, University of Leipzig, Leipzig, Germany
[g] Department of Cognitive Neurology, University of Leipzig, Leipzig, Germany
[h] Department of Electrophysiology, Leipzig Heart Centre, University of Leipzig, Leipzig, Germany
[i] Center for Stroke Research Berlin, Charité – Universitaetsmedizin Berlin, Berlin, Germany

ARTICLE INFO

Keywords:
Heart rate variability
Aging
Eigenvector centrality mapping
Brain structure
Voxel-based morphometry
Default mode network

ABSTRACT

Resting heart rate variability (HRV), an index of parasympathetic cardioregulation and an individual trait marker related to mental and physical health, decreases with age. Previous studies have associated resting HRV with structural and functional properties of the brain – mainly in cortical midline and limbic structures. We hypothesized that aging affects the relationship between resting HRV and brain structure and function. In 388 healthy subjects of three age groups (140 younger: 26.0 ± 4.2 years, 119 middle-aged: 46.3 ± 6.2 years, 129 older: 66.9 ± 4.7 years), gray matter volume (GMV, voxel-based morphometry) and resting state functional connectivity (eigenvector centrality mapping and exploratory seed-based functional connectivity) were related to resting HRV, measured as the root mean square of successive differences (RMSSD). Confirming previous findings, resting HRV decreased with age. For HRV-related GMV, there were no statistically significant differences between the age groups, nor similarities across all age groups. In whole-brain functional connectivity analyses, we found an age-dependent association between resting HRV and eigenvector centrality in the bilateral ventromedial prefrontal cortex (vmPFC), driven by the younger adults. Across all age groups, HRV was positively correlated with network centrality in the bilateral posterior cingulate cortex. Seed-based functional connectivity analysis using the vmPFC cluster revealed an HRV-related cortico-cerebellar network in younger but not in middle-aged or older adults. Our results indicate that the decrease of HRV with age is accompanied by changes in functional connectivity along the cortical midline. This extends our knowledge of brain-body interactions and their changes over the lifespan.

1. Introduction

Behavioral and physiological changes that occur with advancing age become manifest in the structure and function of multiple macro- and micro-systems of the human organism (Arking, 2006). Important alterations occur in the cardiovascular and nervous systems, which are coupled to react dynamically to environmental demands (McEwen, 2003). Such adaptations to internal and external challenges, while leaving an imprint on body and brain, underlie healthy aging (Lipsitz and Goldberger, 1992; Swank, 1996). They are also reflected in brain-heart interactions – particularly in parasympathetic cardioregulation – that can be measured by resting heart rate variability (HRV).

HRV quantifies variations in the cardiac beat-to-beat (or RR) interval that can be measured by electrocardiogram (ECG). Phasic modulation of heart rate (HR) arises from both branches of the autonomic nervous system, the parasympathetic (PNS) and sympathetic (SNS). The PNS quickly reduces HR while the SNS slowly increases it. Some HRV measures represent parasympathetic (i.e., vagal) influences on the heart more

* Corresponding author. Department of Neurology, Max Planck Institute for Human Cognitive and Brain Sciences, Leipzig, Germany.
E-mail address: dkumral@cbs.mpg.de (D. Kumral).

https://doi.org/10.1016/j.neuroimage.2018.10.027
Received 26 June 2018; Received in revised form 5 October 2018; Accepted 9 October 2018
Available online xxxx
1053-8119/

than others (Thayer and Lane, 2007). HRV, typically acquired at rest, is known to decrease with age (De Meersman and Stein, 2007; Umetani et al., 1998). Preservation of autonomic function, as indexed by relatively increased HRV, has been related to longevity and healthy aging (Zulfiqar et al., 2010). Higher HRV has also been associated with better health outcomes (Kemp and Quintana, 2013), for example, with lower risk for cardiovascular diseases (Liao et al., 1997; Thayer et al., 2010) and reduced overall mortality (Buccelletti et al., 2009). In older adults, HRV can indicate inter-individual differences in cognitive performance (Kim et al., 2006; Mahinrad et al., 2016; Zeki Al Hazzouri et al., 2014). Hence, resting HRV could be regarded as a biomarker of healthy aging.

Based on resting state fMRI (i.e., continuous fMRI recordings in the absence of overt task performance or experimental stimulation), spontaneous modulations of the blood oxygenation level dependent (BOLD) signal are used to quantify temporal correlations between brain regions to extract functional connectivity patterns. The number of functional networks in the resting brain is consistent across individuals (Damoiseaux et al., 2006), reliable across time (Shehzad et al., 2009; Zuo et al., 2010), and has been related to inter-individual differences in behavior and cognition (Adelstein et al., 2011; Mennes et al., 2011; Smith et al., 2015). Common ways to examine connectivity patterns of specific brain regions are seed-based functional connectivity analysis (SBCA) or independent component analysis (ICA; Margulies et al., 2010; for a review). Further, graph theory provides a powerful approach to investigate complex brain connectivity patterns (Bullmore and Sporns, 2009; Rubinov and Sporns, 2010). One commonly used measure is eigenvector centrality mapping (ECM). ECM can identify important network nodes (in this case: voxels) based on their functional connectivity (similar to Google's page rank algorithm) without the need to select specific seed regions *a priori* or specify the number of networks/components (Lohmann et al., 2010; Wink et al., 2012). Since ECM focuses on the integration of individual brain regions into the whole brain network, it is a useful whole-brain measure to assess the resting state architecture as it relates to an individual's physiology (García-García et al., 2015; Lohmann et al., 2010), psychology (Koelsch et al., 2013), or health/disease (Binnewijzend et al., 2014; Mueller et al., 2016).

Using such connectivity methods, brain networks associated with autonomic, affective, and cognitive regulation have been identified (Babo-Rebelo et al., 2016; Gould van Praag et al., 2017; Sakaki et al., 2016). One of those is the "central autonomic network" (CAN; Benarroch, 1993), which includes cortical midline structures such as the anterior cingulate cortex (ACC), orbitofrontal cortex (OFC), ventromedial prefrontal cortex (vmPFC), and subcortical areas like the insula, amygdala, and hypothalamus (Beissner et al., 2013; Thayer et al., 2009). With its connections to the sinoatrial node of the heart, via the stellate ganglia and vagus nerve (Beissner et al., 2013; Thayer et al., 2009), the CAN supports visceromotor and neuroendocrine responses that are critical for goal-directed behavior, adaptability, and health (Benarroch, 1993; Hagemann et al., 2003). The "neurovisceral integration model", a framework to explain individual differences in resting vagal function (Kemp et al., 2017; Thayer et al., 2012), extends the role of the CAN in parasympathetic cardioregulation. According to this model, frontal and midbrain areas interact. In particular, the prefrontal cortex (PFC) inhibits subcortical regions and the ANS. Assuming this close interaction of the brain and the ANS in HR regulation, it has been suggested that inter-individual differences in HRV may reflect structural and functional differences in the brain (Thayer et al., 2012). Indeed, resting HRV has been associated with cortical thickness in the right anterior midcingulate cortex (aMCC) in a young sample (Winkelmann et al., 2017). A similar association between cortical thickness and the (rostral anterior) cingulate cortex was found in Yoo et al. (2017), which also included older subjects. The main result of the latter study was an age-invariant association between resting HRV and cortical thickness in ventral brain areas like the lateral OFC (Yoo et al., 2017) (Carnevali et al., 2018 for a review). Another recent study in individuals between 20 and 60 years found a negative correlation between resting HRV and gray matter volume (GMV) in limbic structures such as the insula, amygdala, and parahippocampal gyrus (Wei et al., 2018). Similar brain regions have also been related to HRV in functional neuroimaging studies (Holzman and Bridgett, 2017; Mather and Thayer, 2018; Thayer et al., 2012); both task-based (e.g., BOLD: Critchley et al., 2000; regional cerebral blood flow; rCBF: Gianaros et al., 2004; meta-analyses: Beissner et al., 2013; Thayer et al., 2012) and under resting state conditions (Chang et al., 2013; Jennings et al., 2016; Sakaki et al., 2016). In these studies, activation and connectivity in the medial prefrontal cortex (mPFC), ACC, and posterior cingulate cortex (PCC) have most consistently been associated with HRV and parasympathetic cardioregulation.

Here, we investigated brain-heart interactions across the adult lifespan by combining measures of brain structure and function with the assessment of resting HRV. So far, the only fMRI study that investigated heart-brain interactions on functional connectivity across the adult lifespan included 17 younger and 18 older subjects and restricted their analyses to *a priori* defined regions-of-interest (Sakaki et al., 2016). Across all subjects, higher HRV was related to stronger functional connectivity between the right amygdala and medial prefrontal regions, while age group differences were found in HRV-related connectivity between the right amygdala and lateral prefrontal regions. The main aims of this study were to examine (i) the relationship between resting HRV, brain structure, and functional connectivity as well as (ii) its dependence on age in a large sample of healthy adults across the lifespan. Based on structural and functional findings (reviewed above), we hypothesized that the neural correlates of resting HRV are age-dependent. To detect HRV-related structural alterations, we used voxel-based morphometry (VBM) (Ashburner and Friston, 2000). To assess HRV-related changes in the functional architecture across the whole brain, we used ECM as a data-driven approach, which allows the characterization of whole-brain network architecture without requiring *a priori* assumptions (Lohmann et al., 2010). To further explore age-dependent ECM-derived whole-brain connectivity patterns, we also implemented an exploratory SBCA (for more details see *Methods*).

2. Methods

2.1. Participants

Data from two studies were used: (I) the "Leipzig Research Centre for Civilization Diseases" (LIFE; Loeffler et al., 2015) and (II) the "Leipzig Study for Mind-Body-Emotion Interactions" (LEMON; Babayan et al. in revision).

LIFE is a large population-based cohort study from Leipzig, Germany (Loeffler et al., 2015). From the sample of LIFE subjects with MRI data (n = 2667), we selected healthy subjects between the ages of 20 and 80 years. We applied strict exclusion criteria in three categories: i) health-related criteria; participants were excluded if they reported any medication intake except vitamin food supplements, any past or present cardiovascular health problems, diagnoses, or surgeries, any other medical history and/or diagnosis, in a medical interview. ii) ECG-related criteria (see details on ECG acquisition below); if a subject had more than one ECG recording, we used the first acquired ECG file that was collected on the same day as the MRI acquisition. Otherwise, we selected the ECG recording that was temporally closest to MRI acquisition. Regarding data quality, we excluded data with unrepairable signal artifacts or problems regarding R-peak detection. We also omitted data with any abnormal ECG signal (e.g., supraventricular extrasystoles) after visual inspection as well as subjects with extreme HRV values based on Tukey's (1977) criterion of 3 interquartile ranges (IQR) above the LIFE sample median (N = 14, *Median*: 30.13, IQR: 29.76). iii) MRI-related criteria; we excluded subjects with incidental findings (e.g., brain tumor, multiple sclerosis, or stroke) on T1-weighted and/or fluid-attenuated inversion recovery (FLAIR) images. We further excluded subjects based on rs-fMRI quality assessment, for example with faulty preprocessing (e.g., during denoising) or excessive head motion (criterion: mean framewise

displacement (FD) > 0.6 mm; Power et al., 2015, 2012).

LEMON is a cross-sectional sample of healthy younger and older subjects from Leipzig, Germany, who had never participated in another "psychological or MRI research"-related study, did not report any neurological disorders, head injury, any medication affecting the cardiovascular and/or central nervous system, alcohol or other substance abuse, hypertension, pregnancy, claustrophobia, chemotherapy and malignant diseases, current and/or previous psychiatric disease (Babayan et al. in revision). The LEMON sample comprised 171 eligible subjects divided into two age groups (young: 20–35 years, old: 59–77 years). Similar to the exclusion criteria mentioned above, subjects with incomplete data (N = 38), incidental findings in MRI (FLAIR, T2-weighted, T1-weighted, SWI) (N = 7), or psychoactive drug intake (e.g., tetrahydrocannabinol) determined by urine test (N = 9) were excluded. Two subjects were discarded due to the HRV outlier criterion mentioned above (LEMON sample *Median*: 40.62, IQR: 39.82) and five subjects due to excessive head motion (mean FD > 0.6 mm; Power et al., 2015, 2012). To increase the statistical power and the comparability, we pooled the two samples and divided them into three age groups: young (20-35 years from LIFE and LEMON), middle-aged (35–60 years from LIFE), and old (60-80 years from LIFE and LEMON). Details are provided in Table 1. The participant characteristics separately for each sample and comparing the samples can be found in Supplementary Tables 1-5.

All participants provided written informed consent approved by the ethics committee of the medical faculty at the University of Leipzig, Germany. Both studies were in agreement with the Declaration of Helsinki.

2.2. ECG collection and HRV analysis

LIFE sample. Ten seconds of a standard medical 12-lead resting ECG were acquired using a Page-Writer TC50 ECG system (Philips Medical Systems, Amsterdam, Netherlands) in supine position. The subjects did not receive an explicit instruction before the ECG acquisition. We used lead I (from Einthoven's triangle) for the analysis. R-peaks were automatically detected using the findpeaks function in Matlab 9 (The MathWorks, Inc., Natick, Massachusetts) or Kubios 2.2 (Tarvainen et al., 2014). The ECG data for each subject was manually checked for physiological or computational artifacts like supraventricular extrasystoles or faulty peak detection, respectively. From RR interval time series (i.e., tachograms), we calculated the root mean square of successive differences (RMSSD) of adjacent RR intervals (Task Force of the European Society of Cardiology and the North American Society of Pacing Electrophysiology, 1996; Munoz et al., 2015; Nussinovitch et al., 2011a, 2011b).

LEMON sample. Four minutes of resting ECG were acquired using a Biopac MP35 amplifier with the acquisition software AcqKnowledge version 4.0 (Biopac Systems Inc., http://www.biopac.com, Goleta, CA, USA) and three disposable electrodes on the thorax: the reference electrode was attached near the right collarbone, the measuring electrode on the left-hand side of the body on the same level as the 10th rib, and the ground electrode on the right hip bone. The subjects were instructed to think about daily routines, relax, and breathe at a comfortable rate in sitting position. The peak detection and RMSSD calculation were performed using Kubios 2.2 (Tarvainen et al., 2014).

RMSSD values of our sample were natural log-transformed to obtain normally distributed data (Shapiro-Wilk tests; W = 0.99, p = 0.12). In the following, log-transformed RMSSD will be referred to as "HRV".

2.3. MRI acquisition

Brain imaging for both datasets was performed on the same 3 T Siemens Magnetom Verio MR scanner (Siemens Medical Systems, Erlangen, Germany) with a standard 32-channel head coil. In both samples, subjects were instructed to keep their eyes open and not to fall asleep during the acquisition period.

LIFE sample. The structural T1-weighted images were acquired using a generalized auto-calibrating partially parallel acquisition technique (Griswold et al., 2002) and the Alzheimer's Disease Neuroimaging Initiative standard protocol with the following parameters: inversion time (TI) = 900 ms, repetition time (TR) = 2.3 ms, echo time (TE) = 2.98 ms, flip angle (FA) = 9°, band width = 240 Hz/pixel, field of view (FOV) = 256 × 240 × 176 mm^3, voxel size = 1 × 1 × 1 mm^3, no interpolation. T2*-weighted functional images were acquired using an echo-planar-imaging (EPI) sequence with the following parameters: TR = 2000 ms, TE = 30 ms, FA = 90°, FOV = 192 × 192 × 144 mm^3, voxel size = 3 mm × 3 mm, slice thickness = 4 mm, slice gap = 0.8 mm, 300 vol, duration = 10.04 min. A gradient echo field map with the sample geometry was used for distortion correction (TR = 488 ms, TE 1 = 5.19 ms, TE 2 = 7.65 ms).

LEMON sample. The structural image was recorded using an MP2RAGE sequence (Marques et al., 2010) with the following parameters: TI 1 = 700 ms, TI 2 = 2500 ms, TR = 5000 ms, TE = 2.92 ms, FA 1 = 4°, FA 2 = 5°, band width = 240 Hz/pixel, FOV = 256 × 240 × 176 mm^3, voxel size = 1 × 1 × 1 mm^3. The functional images were acquired using a T2*-weighted multiband EPI sequence with the following parameters: TR = 1400 ms, TE = 30 ms, FA = 69°, FOV = 202 mm, voxel size = 2.3 × 2.3 × 2.3 mm^3, slice thickness = 2.3 mm, slice gap = 0.67 mm, 657 vol, multiband acceleration factor = 4, duration = 15.30 min. A gradient echo field map with the sample geometry was used for distortion correction (TR = 680 ms, TE 1 = 5.19 ms, TE 2 = 7.65 ms).

Table 1
Participant characteristics for each age group. For continuous variables, data is provided in means and standard deviations (in parenthesis). One-way ANOVAs were used to detect age group differences.

	Young (20-35 years)	Middle (35-60 years)	Old (60-80 years)	df	F-value	Eta-squared (η^2)
	(N = 140)	(N = 119)	(N = 129)			
Age (years)	26.01 (4.17)	46.39 (6.25)	66.88 (4.68)			
Sex	38 F/102 M	36 F/83 M	50 F/79 M		4.38[a]	
Resting HRV (RMSSD in ms)	53.35 (27.11)	32.77 (21.01)	27.27 (22.99)	385	43.01***	0.18
Mean HR (1/min)	64.38 (9.62)	62.93 (10.01)	66.24 (10.44)	385	3.41*	0.02
RR interval (ms)	952.56 (137.06)	977.87 (149.75)	928.32 (148.53)	385	3.62*	0.02
mean FD (mm)	0.18 (0.05)	0.28 (0.10)	0.31 (0.11)	385	82.61***	0.30
BMI (kg/m^2)	23.58 (3.03)	26.51 (3.62)	26.54 (3.57)	382	33.34***	0.15
WHR	0.86 (0.07)	0.92 (0.08)	0.95 (0.08)	381	47.64***	0.20
SBP (mmHg)	122.08 (11.42)	126.55 (13.74)	138.76 (18.2)	381	45.45***	0.20
DBP (mmHg)	71.23 (7.33)	78.21 (9.11)	80.00 (10.44)	381	35.47***	0.16
TMT A (s)	24.95 (7.79)	30.33 (12.73)	40.01 (13.54)	384	58.48***	0.23
TMT B (s)	57.72 (17.89)	71.40 (39.04)	95.15 (45.09)	382	45.73***	0.20

*p < 0.05; **p < 0.01; ***p < 0.001, 2-tailed.
[a] Kruskal-Wallis-Test.

2.4. MR data preprocessing and analysis

Structural MRI. We analyzed structural brain alterations on the T1-weighted 3D image using VBM (Ashburner and Friston, 2000) as implemented in SPM12 (Wellcome Trust Centre for Neuroimaging, UCL, London, UK) and the Computational Anatomy Toolbox (CAT12: http://dbm.neuro.uni-jena.de/cat/), running on Matlab 9.3 (Mathworks, Natick, MA, USA). In the LEMON sample before the preprocessing, we removed the background noise from MP2RAGE on the computed uniform images via masking (Streitbürger et al., 2014). The preprocessing steps consisted of segmentation, bias-correction, and normalization using high-dimension Diffeomorphic Anatomical Registration Through Exponentiated Lie Algebra (DARTEL; Ashburner, 2007) with the template from 550 healthy controls of all ages in the IXI Dataset (http://www.brain-development.org) in MNI space. We then applied a 12-parameter affine registration and nonlinear transformation to correct for image size and position. The voxel size was resampled to $1.5 \times 1.5 \times 1.5$ mm and smoothed using an 8-mm Gaussian kernel. For each subject, whole-brain GMV was calculated. An absolute threshold mask of 0.05 was specified in the analyses to cover the whole brain. For quality assessment, we visually inspected the segmentation quality and image homogeneity with the CAT12 toolbox. One participant from the middle-aged group was excluded because of MRI inhomogeneities.

Functional MRI. Preprocessing was implemented in Nipype (Gorgolewski et al., 2011), incorporating tools from FreeSurfer (Fischl, 2012), FSL (Jenkinson et al., 2012), AFNI (Cox, 1996), ANTs (Avants et al., 2011), CBS Tools (Bazin et al., 2014), and Nitime (Rokem et al., 2009). The pipeline comprised the following steps: (I) discarding the first five EPI volumes to allow for signal equilibration and steady state, (II) 3D motion correction (FSL mcflirt), (III) distortion correction (FSL fugue), (IV) rigid body co-registration of functional scans to the individual T1-weighted image (Freesurfer bbregister), (V) denoising including removal of 24 motion parameters (CPAC, Friston et al., 1996), motion, signal intensity spikes (Nipype rapidart), physiological noise in white matter and cerebrospinal fluid (CSF) (CompCor; Behzadi et al., 2007), together with linear and quadratic signal trends, (VI) band-pass filtering between 0.01 and 0.1 Hz (Nilearn), (VII) spatial normalization to MNI152 standard space (3 mm isotropic) via transformation parameters derived during structural preprocessing (ANTS). (VIII) The data were then spatially smoothed with a 6-mm FWHM Gaussian kernel.

The reproducible workflows containing all implementation details for our datasets can be found here: LIFE; https://github.com/fliem/LIFE_RS_preprocessing, LEMON; https://github.com/NeuroanatomyAndConnectivity/pipelines/releases/tag/v2.0.

Eigenvector Centrality Mapping (ECM). In ECM, each voxel in the brain receives a centrality value that is larger if the voxel is strongly correlated with many other voxels that are themselves central (Lohmann et al., 2010). Higher EC values thus indicate stronger connectedness of the respective area (Lohmann et al., 2010; Wink et al., 2012). ECM is computationally efficient, enables connectivity analysis at the voxel level, and does not require initial thresholding of connections (Lohmann et al., 2010). Here, the fast ECM implementation was used (Wink et al., 2012). We restricted our ECM analysis to GM, which we extracted with a mask from the tissue priors in SPM12 by selecting voxels with a GM tissue probability of 20% or higher. The resulting mask contained ~63,000 voxels covering the entire brain.

Exploratory Seed-based Functional Connectivity Analysis (SBCA). To further explore the connectivity patterns of significant age-dependent centrality changes across the whole brain, ECM was complemented by SBCA. Regions detected in ECM can be used as seeds in a subsequent SBCA to investigate intrinsic functional connectivity patterns (Taubert et al., 2011). A bilateral vmPFC seed was created by binarizing the significant ECM findings (MNI coordinates: [$x = 0$, $y = 57$, $z = -6$], cluster size $k = 62$). Time series were extracted and averaged across all voxels of the seed. For each subject, a correlation between the time series of the seed and every other voxel in the brain was calculated using 3dfim+ (AFNI). The resulting correlation maps were Fisher r-to-z transformed using 3dcalc (AFNI).

Statistical analyses for f/MRI. Statistical analyses were carried out using the general linear model (GLM) approach implemented in SPM12. For all analyses, we used resting HRV as the variable of interest and age, sex, study, and either total intracranial volume (TIV, for VBM analysis) or in-scanner head motion (mean FD; Power et al., 2015, 2012 for ECM and SBCA) as covariates of no interest. We performed a one-way ANOVA with three age groups (young, middle, and old) as between-subject factor and calculated the interaction effect between HRV and age group. Based on the significant results of the ANOVA, we computed pairwise group differences using independent t-tests. Using one-sample t-tests, we further tested the main effect of HRV across all subjects and for each age group separately.

As additional controls, (1) both samples were analyzed separately (for more details see Supplementary Table 7), (2) HRV analyses were repeated using resting HR – instead of HRV – as variable of interest and age, sex, study, and either TIV (for VBM) or mean FD (for ECM and SBCA) as covariates of no interest, as well as (3) the effect of age on EC maps – controlling for sex, study, and mean FD (Long et al., 2017; Zuo et al., 2012).

For each statistical analysis, a positive and a negative contrast were computed. Only results surviving whole-brain family-wise error (FWE) correction at $p < 0.05$ (cluster-level) with a voxel-level threshold of $p < 0.001$ were considered significant. All (unthresholded) statistical maps are available at NeuroVault (Gorgolewski et al., 2015) for detailed inspection in 3D (http://neurovault.org/collections/TELEUIIY).

2.5. Potential confounding factors for HRV

Sex. As HRV has been reported to differ between sexes (Koenig and Thayer, 2016; Voss et al., 2015; Thayer et al., 2015), we analyzed sex differences in HRV per age group in a 2 (sex) × 3 (age group) ANOVA.

Smoking. Since smoking has a short- and long-term impact on HRV (Felber Dietrich et al., 2007; Hayano et al., 1990), we examined potential effects of smoking status on HRV. To this end, we classified subjects into three groups (smokers: $N = 75$, former smokers: $N = 84$, and non-smokers: $N = 220$, [no info available: $NA = 9$]). We used a 2 (sex) x 3 (smoking) ANOVA to test the mean differences between the groups using sex as additional between-subjects factor.

Blood Pressure. Systolic blood pressure (SBP) and diastolic blood pressure (DBP) were measured in a seated position using an automatic oscillometric blood pressure (BP) monitor (LIFE sample; OMRON 705IT, LEMON sample; OMRON M500) after a resting period of 5 min. While in the LIFE sample three consecutive BP measurements were taken from the right arm in intervals of 3 min, in the LEMON sample measurements were taken from participants' left arms on three separate occasions within two weeks. In each sample, all available measurements per participant were averaged to one SBP and one DBP value.

Anthropometric measurements. Subjects' heights and weights were taken according to a standardized protocol by trained study staff. Body mass index (BMI; in kg/m^2) was calculated by dividing the body weight by the square of the body height, while waist to hip ratio (WHR) was calculated as waist circumference measurement divided by hip circumference measurement (Huxley et al., 2010). As a control, all analyses on the association between HRV and the brain across the age groups were repeated with BP and BMI as additional covariates of no interest.

Cognition. Previous studies have related resting HRV to cognitive performance (Hansen et al., 2004; Mahinrad et al., 2016; Zeki Al Hazzouri et al., 2014). The latter is often assessed using the Trail Making Test (TMT), which measures executive function, processing speed, or mental flexibility (Reitan, 1955; Reitan and Wolfson, 1995). By drawing lines, subjects sequentially connect numbers and/or letters while their reaction times are recorded. In the first part of the test (TMT-A) the targets are all numbers (1, 2, 3, etc.), while in the second part (TMT-B), participants need to alternate between numbers and letters (1, A, 2, B, etc.). In both

TMT A and B, the time to complete the task quantifies the performance and lower scores indicate better performance.

For cognition, BP, and anthropometric measurements, we assessed age-group differences statistically using one-way ANOVAs and then tested their association with HRV using Spearman correlations for each age group. To determine statistical significance, we used a two-sided α-level of 0.05. Statistical analyses were conducted using R version 3.3.2 (R Core Team, 2016).

3. Results

Details about the demographic, anthropometric, cardiovascular, and cognitive characteristics of the 388 participants can be found in Table 1. The age groups differed significantly on all variables (Table 1). Compared to population-based norms (Hobert et al., 2011; Then et al., 2014; Tombaugh, 2004), our sample shows higher TMT scores, indicating cognitive health.

Note. HRV = heart rate variability; RMSSD = root mean square of successive differences; HR = heart rate, FD = framewise displacement; BMI = body mass index; WHR = waist to hip ratio; SBP = systolic blood pressure; DBP = diastolic blood pressure; TMT = trail making test.

There was a significant main effect of age group ($F(2,382) = 63.552$, $p = 2 \times 10^{-16}$, $\eta^2 = 0.182$), no significant main effect of sex ($F(1,382) = 0.187$, $p = 0.666$), and no significant age group × sex interaction on HRV ($F(2,382) = 0.233$, $p = 0.792$). HRV did not differ as a function of smoking status (main effect smoking group: $F(2,373) = 1.241$, $p = 0.290$, main effect of sex: $F(1,373) = 0.473$, $p = 0.492$; smoking group × sex interaction: $F(2,373) = 0.606$, $p = 0.546$).

HRV was negatively correlated with age (rho = −0.210, p = 0.010), BMI (rho = −0.207, p = 0.020), and DBP (rho = −0.231, p = 0.012) in the middle-aged individuals. No significant associations were found between HRV and mean FD, SBP, WHR, TMT A, or TMT B in any of the age groups (Supplementary Table 6).

Voxel-based Morphometry (VBM). There was no significant association between HRV and GMV across all subjects. Also, an ANOVA did not yield a significant age group × HRV interaction on GMV. While an exploratory one-sample *t*-test in the middle-aged group indicated a significant HRV-related increase of GMV in the left cerebellum (MNI coordinates: [-15, −87, −51], k = 1540, T = 3.92, pFWE = 0.004), there were no significant effects of HRV on GMV for younger and older adults. Control analyses that included BP and BMI as covariates of no interest did not change the results (https://neurovault.org/collections/TELEUIIY/). Additional analyses using resting HR as covariates of interest did not show any significant VBM results neither across all age groups, nor in each age group (https://neurovault.org/collections/TELEUIIY/).

Eigenvector Centrality Mapping (ECM). A significant effect of age group on the relation between resting HRV and EC was detected in the bilateral

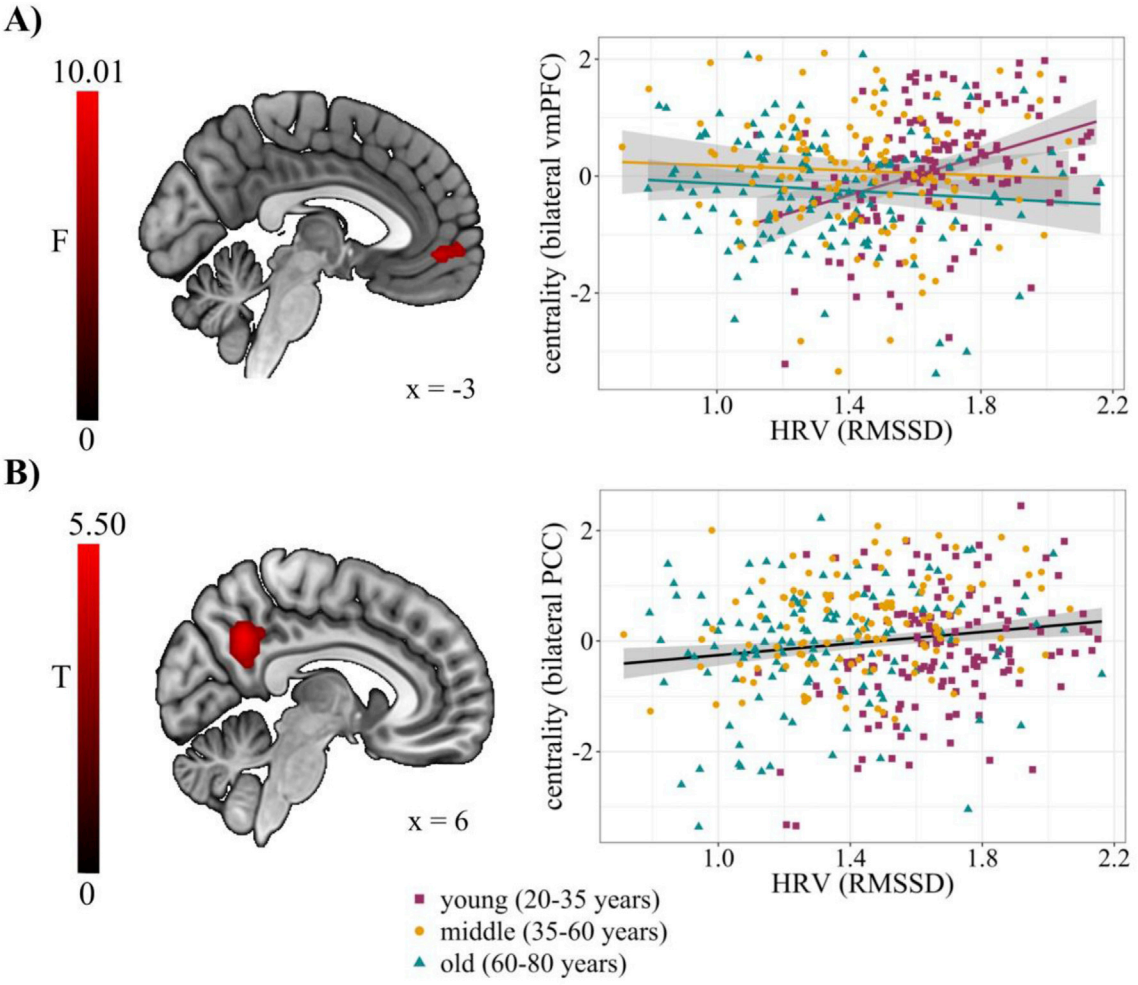

Fig. 1. Association between resting heart rate variability (HRV), measured as root mean square of successive differences (RMSSD), and eigenvector centrality (EC). **A)** The interaction between age group and HRV was significant in the bilateral ventromedial prefrontal cortex (vmPFC; MNI coordinates: [0, 57, −6], k = 62, F = 10.79, pFWE = 0.006), displayed at x = −3. **B)** An increased EC in the bilateral posterior cingulate cortex (PCC; MNI coordinates [6, −54, 36], k = 204, T = 5.29, pFWE < 0.001) across all age groups, displayed at x = 6. Threshold: $p < 0.001$ at the voxel and $p < 0.05$ with family-wise error (FWE) correction at the cluster level.

vmPFC (MNI coordinates: [0, 57, −6], k = 62, F = 10.79). The resulting beta values for each age group are plotted in Fig. 1A, suggesting that younger adults show a stronger positive association between HRV and EC in the bilateral vmPFC than middle-aged and older individuals (Table 2). This was supported by post-hoc two-sample t-tests, which indicated that the correlation between HRV and EC in the bilateral vmPFC was significantly stronger for young > old and young > middle-age subjects (Table 2). A one-sample *t*-test across all subjects showed increased EC with higher HRV in the bilateral PCC (Fig. 1B). The negative contrast did not yield any significant results. In separate one-sample t-tests for each age group, we found HRV-dependent EC increases in the right vmPFC, bilateral PCC, and superior frontal gyrus (SFG), as well as HRV-dependent EC decreases in the left superior occipital gyrus (SOG) including the cuneus and calcarine sulcus in the group of young subjects. Our data did not show any significant positive or negative correlation with HRV in the groups of middle-aged and old subjects that were correctable for multiple comparisons. The complete ECM results are presented in Table 2.

Control analyses that included BP and BMI as covariates of no interest did not change the results (https://neurovault.org/collections/TELEUIIY/). Resting HR – instead of HRV –was not significantly associated with functional brain centrality, neither across all age groups, nor in each age group separately (https://neurovault.org/collections/TELEUIIY/). The association between age and EC is shown in Supplementary Figure 1.

Exploratory Seed-based Functional Connectivity Analysis (SBCA). In the additional exploratory SBCA, a significant effect of age group on the relation between resting HRV and whole-brain bilateral vmPFC connectivity was found in the bilateral cerebellum, right superior parietal lobe (SPL), left middle occipital gyrus (MOG), inferior occipital gyrus (IOG), and left SFG extended to the supplementary motor area (SMA). The beta values from the right cerebellum for each age group are plotted in Fig. 2A, suggesting that younger adults show stronger functional connectivity between the bilateral vmPFC and right cerebellum than middle-aged and older individuals (Table 3). The post-hoc two-sample t-tests similarly indicated that higher HRV levels were significantly correlated with stronger functional connectivity between the bilateral vmPFC and cerebellum, right SPL, left MOG, left post-central gyrus, and left SMA for the contrasts of young > old and young > middle (Table 3). A one-sample *t*-test in the overall sample, to assess the association between HRV and bilateral vmPFC connectivity, showed an increased functional connectivity with the left middle frontal gyrus (MFG) extending to the dorsolateral prefrontal cortex (DLPFC) (Fig. 2B). Separate one-sample t-tests for each age group showed no significant association for the middle-aged and older subjects but an increased vmPFC connectivity in distributed brain regions including the bilateral cerebellum, bilateral MOG, and the right SMA for the young subjects. We did not observe any significant negative correlations, neither in the overall sample nor in each age group. Control analyses that included BP and BMI as covariates of no interest did not change the results (https://neurovault.org/collections/TELEUIIY/). The complete SBCA results are presented in Table 3.

4. Discussion

In the present study, we assessed the relationship between parasympathetic cardioregulation (indexed by HRV) and brain structure (using VBM) as well as whole-brain resting state functional connectivity (using ECM and SBCA) in a large sample of healthy young, middle-aged,

Table 2
Brain regions that show significant increases or decreases in eigenvector centrality with resting heart rate variability (HRV). Threshold: $p < 0.001$ at the voxel and $p < 0.05$ with family-wise error (FWE) correction at the cluster level.

	Regions	H	cluster size k (Voxel)	MNI coordinates			FWE	z	F/T-value
				x	y	z			
ANOVA	Ventromedial prefrontal cortex	R/L	62	0	57	−6	0.006	4.03	10.79
				−3	48	−6		3.76	9.63
				0	60	3		3.49	8.53
Across age groups (+)	Posterior cingulate cortex/precuneus	R/L	204	6	−54	36	<0.001	5.29	5.39
				−9	−57	33		4.04	4.09
				−12	−51	45		3.35	3.38
Young (+)	Ventromedial prefrontal cortex	R	316	0	57	−6	<0.001	5.07	5.16
				6	51	9		4.89	4.98
				15	60	15		4.22	4.16
	Posterior cingulate cortex/precuneus	R/L	167	6	−57	27	<0.001	4.46	4.52
				−9	−54	18		3.72	3.75
				−9	−60	27		3.70	3.74
	Superior frontal gyrus	R/L	240	15	33	48	0.002	4.50	4.56
				15	48	39		4.32	4.37
				−6	36	48		4.24	4.29
Young (−)	Superior occipital gyrus	L	129	−6	−96	3	<0.001	4.63	4.70
				−15	−99	−3		4.24	4.29
				0	−84	−3		3.71	3.76
Middle (+)	n.s								
Middle (−)	n.s								
Old (+)	n.s								
Old (−)	n.s								
Young > Old	Ventromedial prefrontal cortex	R/L	131	0	57	−6	<0.001	4.45	4.51
				0	60	3		4.01	4.05
				−3	45	−8		3.62	3.65
Young < Old	n.s								
Middle > Young	n.s								
Middle < Young	Ventromedial prefrontal cortex	R/L	85	3	45	−6	0.005	4.09	4.13
				−12	48	−9		4.06	4.11
				6	45	15		3.58	3.61
Old > Middle	n.s								
Old < Middle	n.s								

Note. R = right, L = left, H = hemisphere, ANOVA = analysis of variance, MNI = Montreal Neurological Institute, n.s = not significant.

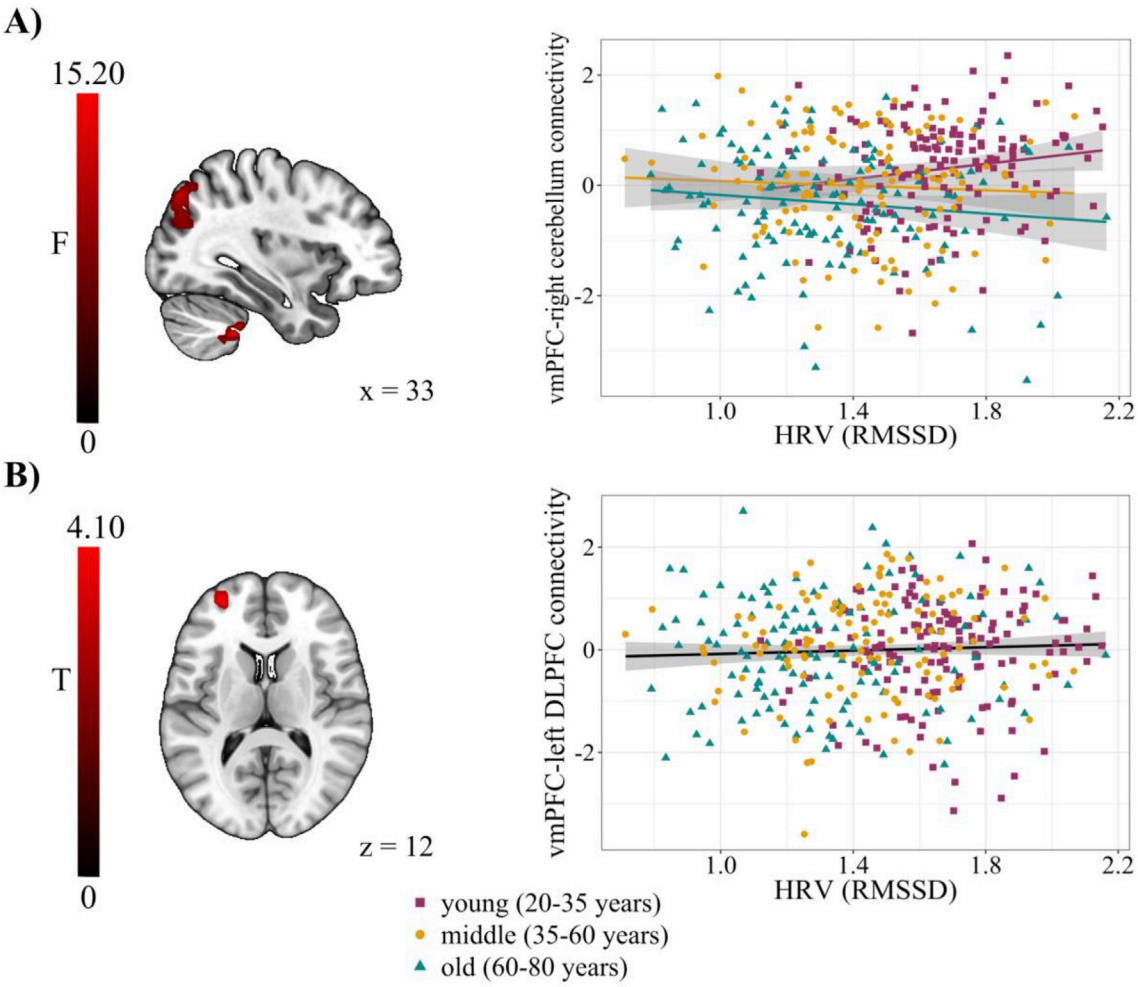

Fig. 2. Association between resting heart rate variability (HRV), measured as root mean square of successive differences (RMSSD), and brain function in an exploratory seed-based functional connectivity analysis originating from the bilateral ventromedial prefrontal cortex (vmPFC). **A)** The interaction between age group and HRV was significant in the right cerebellum (MNI coordinates [33, −42, −45], $k = 46$, $F = 15.19$, $pFWE < 0.001$), displayed at $x = 33$. **B)** An increased functional connectivity in the right dorsolateral prefrontal cortex (DLPFC; MNI coordinates [-30, 54, 12], $k = 67$, $T = 4.10$, $pFWE = 0.032$) was found across all age groups, displayed at $z = 12$. Threshold: $p < 0.001$ at the voxel and $p < 0.05$ with family-wise error (FWE) correction at the cluster level.

and older participants. We used an optimally healthy sample for a given age range in terms of both physical (e.g., Janssen et al., 2002) and cognitive health (e.g., Hobert et al., 2011; Tombaugh, 2004). We found the frequently observed age-related decrease in resting HRV (Almeida--Santos et al., 2016; Voss et al., 2015) to be accompanied by age-dependent and age-invariant alterations in brain function. Specifically, higher HRV was linked to stronger network centrality in several brain regions, particularly along the cortical midline. In the PCC, this correlation was present in all age groups while in the vmPFC, network centrality was related to higher HRV in young but not in middle-aged and old adults. These findings support the view that altered HRV during aging may have a functional brain component associated with it.

4.1. *Age-dependent association of resting HRV with functional connectivity*

Given the relationship between HRV and age (Almeida-Santos et al., 2016; Voss et al., 2015), HRV and brain structure (Wei et al., 2018), as well as HRV and brain function (Sakaki et al., 2016), we hypothesized the neural correlates of resting HRV to be also age-dependent. Our results confirm that the relationship between HRV and network centrality at rest differs between age groups. Evidence is accumulating that alterations of intrinsic brain activity are a key feature of normal brain aging (Damoiseaux et al., 2008). Age-dependent intrinsic connectivity alterations in the DMN have been found not only in healthy aging (Ferreira and Busatto, 2013) but also in age-related pathologies, for example, in individuals with a high familial risk for depression (Posner et al., 2016) and in young APOE-ε4 carriers (Filippini et al., 2009), which is a possible biomarker for Alzheimer's dementia (Kanekiyo et al., 2014). Our finding that resting HRV is related to increased network centrality in medial frontal regions in the young but not in the middle-aged or old age group could be interpreted in the framework of the functional plasticity hypothesis of cognitive aging (Greenwood, 2007). According to this hypothesis, the structural vulnerability – particularly of prefrontal cortex – leads to an age-related functional reorganization (e.g., Grady, 2012; for a review). The changes in the resting state network architecture around the vmPFC that are related to parasympathetic cardioregulation could thus represent altered cardiovascular control with advancing age and concomitant network reorganization.

In addition to the age-dependent association of resting HRV with functional brain network centrality in medial frontal regions, we also found an HRV-related bilateral medial parietal cluster in the PCC that was independent of age. Both vmPFC and PCC are central nodes of the CAN (Benarroch, 1993) and the DMN (Greicius et al., 2003; Uddin et al., 2009) and have been related to self-generated or internally directed mental processes like thoughts and feelings (Andrews-Hanna et al., 2014; Raichle et al., 2001). The medial frontal (e.g., vmPFC) and medial

Table 3
Brain regions that show resting heart rate variability-related connectivity with the bilateral ventromedial prefrontal cortex (vmPFC) in an exploratory seed-based functional connectivity analysis. Thresholds: $p < 0.001$ at the voxel and $p < 0.05$ with family-wise error (FWE) correction at the cluster level.

	Regions	H	cluster size k (Voxels)	MNI coordinates			FWE	z	F/T- value
				x	y	z			
ANOVA	Cerebellum	R	46	33	−42	−45	0.049	4.91	15.19
	Superior parietal lobe	R	203	24	−75	51	<0.001	4.48	12.94
				33	−78	45		4.34	12.25
				36	−75	30		3.82	9.88
	Middle occipital gyrus	L	57	−33	−84	30	0.021	4.24	11.74
				−39	−66	24		3.31	7.84
	Inferior occipital gyrus		60	−33	−69	−6	0.016	3.85	9.97
				−42	−63	−3		3.76	9.61
				−51	−69	−15		3.62	9.03
	Cerebellum	L	61	−30	−60	−30	0.015	3.83	9.91
				−33	−66	−21		3.59	8.91
				−39	−72	−18		3.58	8.87
	Superior frontal gyrus extended to supplementary motor area	R/ L	71	0	15	66	0.007	3.73	9.47
				0	3	57		3.6	8.96
				9	12	57		3.53	8.66
Across age groups (+)	Middle frontal gyrus extended to dorsolateral prefrontal cortex	L	67	−30	54	12	0.032	4.06	4.10
				−36	54	3		3.54	3.57
				−18	51	3		3.39	3.42
Young (+)	Cerebellum	R	131	33	−42	−45	0.001	5.06	5.15
				42	−60	−48		4.68	4.75
				36	−63	−39		3.29	3.31
	Cerebellum	L	116	−12	−57	−54	0.002	4.6	4.67
				−21	−69	−54		4.2	4.25
				−15	−48	−51		4.09	4.14
	Middle occipital gyrus	R	163	39	−75	42	<0.001	4.46	4.52
				30	−69	51		4.15	4.20
				21	−78	51		3.63	3.67
	Middle occipital gyrus	L	131	−39	−66	24	0.001	4.31	4.37
				−33	−84	30		3.94	3.98
				−39	−60	12		3.47	3.50
	Cerebellum	R	63	18	−75	−18	0.04	4.13	4.18
				27	−81	−18		3.68	3.72
				18	−84	−15		3.64	3.67
	Cerebellum	L	102	−33	−81	−21	0.005	4.13	4.18
				−30	−60	−30		3.7	3.74
				−21	−90	−15		3.59	3.62
	Supplementary motor area	R	87	3	6	54	0.01	3.77	3.81
				0	15	69		3.68	3.72
				9	12	57		3.59	3.63
Young (−)	n.s								
Middle (+)	n.s								
Middle (−)	n.s								
Old (+)	n.s								
Old (−)	n.s								
Young > Old	Cerebellum	R	67	33	−42	−45	0.032	4.59	4.66
				15	−48	−51		3.63	3.67
				27	−57	−45		3.41	3.44
	Inferior occipital gyrus	L	237	−33	−69	−6	<0.001	4.41	4.47
				−42	−63	−3		4.33	4.38
				−39	−72	−18		4.14	4.19
	Superior parietal lobe	R	275	24	−78	51	<0.001	4.31	4.37
				36	−75	45		4.21	4.26
				36	−75	27		3.95	4.00
	Middle occipital gyrus	L	140	−27	−84	27	0.001	4.30	4.35
				−36	−66	24		3.89	3.93
				−39	−60	12		3.62	3.65
	Superior frontal gyrus extended to supplementary motor area	R/ L	147	−3	3	57	0.001	3.99	4.04
				12	6	63		3.72	3.75
				3	12	66		3.61	3.65
	Postcentral gyrus	R	72	42	−6	30	0.024	3.87	3.91
				54	6	24		3.69	3.73
				54	0	33		3.53	3.56
	Superior frontal gyrus extended to supplementary motor area	R/ L	73	3	−18	60	0.022	3.62	3.66
				−3	−36	69		3.56	3.59
				3	−9	69		3.29	3.31
Young < Old	n.s								
Middle > Young	n.s								
Middle < Young	Cerebellum	R	189	33	−42	−45	<0.001	4.99	5.08
				42	−60	−48		4.60	4.67

(*continued on next page*)

Table 3 (*continued*)

	Regions	H	cluster size k (Voxels)	MNI coordinates			FWE	z	F/T- value
				x	y	z			
				18	−45	−51		4.34	4.40
	Superior parietal lobe	R	270	27	−72	51	<0.001	4.76	4.83
				33	−78	45		4.51	4.58
				36	−75	30		4.04	4.09
	Cerebellum	L	239	−12	−57	−54	<0.001	4.74	4.82
				−15	−45	−51		4.61	4.68
				−12	−39	−45		4.36	4.42
	Middle occipital gyrus	L	76	−33	−84	30	0.019	4.59	4.66
				−45	−72	27		3.37	3.40
	Cerebellum	R/L	313	−30	−60	−30	<0.001	4.27	4.32
				12	−69	−21		4.18	4.23
				18	−78	−18		3.95	3.99
	Superior frontal gyrus extended to supplementary motor Area	L	109	0	15	66	0.003	4.19	4.24
				15	9	69		3.61	3.64
Old > Middle	n.s								
Old < Middle	n.s								

Note. R = right, L = left, H = hemisphere, ANOVA = analysis of variance, MNI = Montreal Neurological Institute.

parietal components (e.g., PCC and precuneus) of CAN and DMN have been particularly implied in parasympathetic functioning (Beissner et al., 2013; Benarroch, 1993). In addition, prefrontal visceral structures (Price, 2007, 1999) respond to heartbeats (Babo-Rebelo et al., 2016; Park et al., 2014) and modulate HR or HRV (Makovac et al., 2017; Van Eden and Buijs, 2000). It is plausible that in the absence of external stimulation, brain function (i.e., activity and connectivity) in CAN and DMN is predominantly allocated to the "internal milieu", that is, to monitoring and regulating bodily signals (e.g., the parasympathetic "rest-and-digest"). Fittingly, the PCC has been found active in tasks that involved the assessment of self-relevance (Yu et al., 2011) as well as self-location and body ownership (Guterstam et al., 2015), while the vmPFC was related to processing bodily information (Gusnard et al., 2001), autonomic control (Critchley et al., 2011), and cardiovascular arousal (Wong et al., 2007).

Using the cluster that showed a significant interaction in the centrality analyses, the exploratory SBCA similarly showed an age-dependent relationship between resting HRV and functional brain connectivity. Specifically, we found stronger functional connectivity between the bilateral vmPFC and a widespread set of brain regions including the bilateral cerebellum, bilateral occipital gyrus, right SPL, and bilateral SFG extending to the SMA in young but not in middle-aged or older adults. These results extend the ECM findings by suggesting additional cortico-cerebellar regions might be involved in the modulation of visceral processes. In line with this interpretation, activation in the cerebellum has been connected to the regulation of visceral responses (Demirtas-Tatlidede et al., 2011), fear conditioning (Leaton, 2003; Sacchetti et al., 2002), feeding (Tataranni et al., 1999), as well as the coordination and control of cardiovascular activities (Bradley et al., 1991; Ghelarducci and Sebastiani, 1996). Furthermore, autonomic activity during cognitive and motor tasks was positively associated with activation in the cerebellum and, among other regions, the SMA and dorsal ACC (Critchley et al., 2003).

Despite previous evidence of the relationship between GMV and vagally-mediated HRV in CAN regions (Wei et al., 2018), using whole-brain VBM analysis, we only found a significant GMV change related with resting HRV in the cerebellum for the middle-aged group. Notably, in the study by Wei et al. (2018), reduced GM volume in the cerebellum was associated with HR (but not HRV) in healthy middle-aged individuals. However, using resting HR, we were also not able to replicate the previous findings (Wei et al., 2018). The divergent results could be due to different measurement parameters (e.g., MRI sequence parameters) but also to different effect size or statistical power (for more details see *Limitations*).

Finally, while our study investigated the neural correlates of resting HRV, previous studies investigated the neural correlates of HR at rest and HR changes with stimulation or tasks (e.g., Beissner et al., 2013 for a review). Our additional analyses using resting HR as covariate of interest did not show significant associations with brain structure or function. This suggests that resting HRV and resting HR (as they are differentially influenced by the branches of the ANS) have different neural components at rest.

4.2. Physiological and psychophysiological interpretations of HRV

The most fundamental (purely physiological) understanding of the role of the ANS – and particularly the PNS – is to ensure visceral and cardiovascular functioning or bodily homeostasis by allowing rapid adaptive behavioral and physiological reactions in ever-changing environments, or by disengagement and relaxation in resting moments ("rest-and-digest"; e.g., Cannon, 1929). More *psycho*physiological interpretations of ANS function have extended this view to cognitive, affective, and social phenomena. For example, the neurovisceral integration model takes higher HRV to facilitate physiological, cognitive, socio-emotional, and behavioral flexibility or adaptation (Smith et al., 2017; Thayer and Lane, 2000; Thayer and Ruiz-Padial, 2006). It explicitly links the brain and the rest of the body by assuming that the PFC – and particularly the vmPFC – tonically inhibits the amygdala, which affects autonomic function, thereby linking both nervous systems to inhibitory or self-regulatory processes (Holzman and Bridgett, 2017; Kemp et al., 2017; Thayer et al., 2012). Convergently, resting HRV has recently been associated with vmPFC activation during a dietary self-control task in young adults (Maier and Hare, 2017).

5. Limitations

There are a number of limitations that should be considered in the interpretation of our results. The study design is cross-sectional and does not allow us to infer the directionality of the association between resting HRV and the brain. Additionally, our health criteria also allowed inclusion of subjects with higher BMI (>25 kg/m^2) or untreated/undiagnosed hypertension (SBP > 140 mmHg, DBP > 90 mmHg). This makes it difficult to disentangle HRV-related influences from other bodily/cardiovascular influences, which are also physiologically related (BMI: Molfino et al., 2009; BP: Singh et al., 1998). However, control analyses that accounted for BP and BMI showed very similar results of the association between resting HRV and the brain. Although psychological interpretations of a single physiological marker like resting HRV are intrinsically limited, previous studies have associated HRV with different

trait or state levels of, for example, executive control (Capuana et al., 2014), stress (Sin et al., 2016), and emotion regulation (Williams et al., 2015). For a psychological interpretation of our finding that the association between HRV and functional connectivity at rest is age-dependent, similar analyses on task-related parasympathetic and neural activity could be helpful. The samples differed significantly, for example in resting HRV (young subjects), sex distribution, sample size, BP, and MRI/ECG acquisition parameters (Supplementary Table 1, Tables 4 and 5). Although we accounted for within- and between-sample variance in the second-level GLM, these differences may still have influenced our results (e.g., for structural MRI; Streitbürger et al., 2014). Further, we calculated the RMSSD using 10 s of ECG data, which has been shown to be a valid measurement (Munoz et al., 2015; Nussinovitch et al., 2011a, 2011b). Nevertheless, ECG data recorded over longer periods (e.g., 24-h) can complement this "ultra-short" evaluation of parasympathetic function. Finally, although ECM is a relatively new measure that has certain advantages (see above and Lohmann et al., 2010; Wink et al., 2012), studies using other measures of functional connectivity could complement our findings on the association of parasympathetic cardioregulation and functional brain connectivity.

6. Conclusion

In this cross-sectional study, we examined the association of resting HRV with brain structure and functional connectivity in different age groups of healthy adults. Our main findings are correlations between resting HRV and brain network architecture in the PCC across all age groups and in the vmPFC in young but not in middle-aged or older subjects. These support the view that the well-known HRV decrease with age may have a functional brain network component along the cortical midline. Consistent with the role of these areas in affective, cognitive, and autonomic regulation, our results provide a comprehensive picture of the differential effect of aging on heart-brain interactions. These findings emphasize the importance of parasympathetic cardioregulation in healthy aging.

Financial disclosures

The authors declare no conflict of interest.

Acknowledgments

This study was supported by LIFE Leipzig Research Center for Civilization Diseases at the University of Leipzig funded by the European Union, European Regional Development Fund, and the Free State of Saxony. The authors would like to thank all volunteers for their participation in one of the two studies. Further, we thank all researchers, technicians and students who planned, collected, entered and curated data, used in this manuscript.

Appendix A. Supplementary data

Supplementary data related to this article can be found at https://doi.org/10.1016/j.neuroimage.2018.10.027.

References

Adelstein, J.S., Shehzad, Z., Mennes, M., DeYoung, C.G., Zuo, X.N., Kelly, C., Margulies, D.S., Bloomfield, A., Gray, J.R., Castellanos, F.X., Milham, M.P., 2011. Personality is reflected in the brain's intrinsic functional architecture. PloS One 6. https://doi.org/10.1371/journal.pone.0027633.

Almeida-Santos, M.A., Barreto-Filho, J.A., Oliveira, J.L.M., Reis, F.P., da Cunha Oliveira, C.C., Sousa, A.C.S., 2016. Aging, heart rate variability and patterns of autonomic regulation of the heart. Arch. Gerontol. Geriatr. 63, 1–8. https://doi.org/10.1016/j.archger.2015.11.011.

Andrews-Hanna, J.R., Smallwood, J., Spreng, R.N., 2014. The default network and self-generated thought: component processes, dynamic control, and clinical relevance. Ann. N. Y. Acad. Sci. 1316, 29–52. https://doi.org/10.1111/nyas.12360.

Arking, R., 2006. The biology of aging: observations and principles. The Biology of Aging Observations Principles. https://doi.org/10.1080/03601270701498491.

Ashburner, J., 2007. A fast diffeomorphic image registration algorithm. Neuroimage 38, 95–113. https://doi.org/10.1016/j.neuroimage.2007.07.007.

Ashburner, J., Friston, K.J., 2000. Voxel-based morphometry—the methods. Neuroimage 11, 805–821. https://doi.org/10.1006/nimg.2000.0582.

Avants, B.B., Tustison, N.J., Song, G., Cook, P.A., Klein, A., Gee, J.C., 2011. A reproducible evaluation of ANTs similarity metric performance in brain image registration. Neuroimage 54, 2033–2044. https://doi.org/10.1016/j.neuroimage.2010.09.025.

Babayan, A., Erbey, M., Kumral, D., Reinelt, R. D., Reiter, A. M. F., Röbbig, J., Schaare, L. H., Uhlig, M., et al., A Mind-brain-body Dataset of MRI, EEG, Cognition, Emotion, and Peripheral Physiology in Young and Old Adults, (in revision).

Babo-Rebelo, M., Wolpert, N., Adam, C., Hasboun, D., Tallon-Baudry, C., 2016. Is the cardiac monitoring function related to the self in both the default network and right anterior insula? Philos. Trans. R. Soc. B Biol. Sci. 371 https://doi.org/10.1098/rstb.2016.0004, 20160004.

Bazin, P.L., Weiss, M., Dinse, J., Schäfer, A., Trampel, R., Turner, R., 2014. A computational framework for ultra-high resolution cortical segmentation at 7 Tesla. Neuroimage 93, 201–209. https://doi.org/10.1016/j.neuroimage.2013.03.077.

Behzadi, Y., Restom, K., Liau, J., Liu, T.T., 2007. A component based noise correction method (CompCor) for BOLD and perfusion based fMRI. Neuroimage 37, 90–101. https://doi.org/10.1016/j.neuroimage.2007.04.042.

Beissner, F., Meissner, K., Bar, K.-J., Napadow, V., 2013. The autonomic brain: an activation likelihood estimation meta-analysis for central processing of autonomic function. J. Neurosci. 33, 10503–10511. https://doi.org/10.1523/JNEUROSCI.1103-13.2013.

Benarroch, E.E., 1993. The central autonomic network: functional organization, dysfunction, and perspective. Mayo Clin. Proc. 68, 988–1001. https://doi.org/10.1016/S0025-6196(12)62272-1.

Binnewijzend, M.A.A., Adriaanse, S.M., Van der Flier, W.M., Teunissen, C.E., de Munck, J.C., Stam, C.J., Scheltens, P., van Berckel, B.N.M., Barkhof, F., Wink, A.M., 2014. Brain network alterations in Alzheimer's disease measured by Eigenvector centrality in fMRI are related to cognition and CSF biomarkers. Hum. Brain Mapp. 35, 2383–2393. https://doi.org/10.1002/hbm.22335.

Bradley, D.J., Ghelarducci, B., Spyer, K.M., 1991. The role of the posterior cerebellar vermis in cardiovascular control. Neurosci. Res. 12, 45–56. https://doi.org/10.1016/0168-0102(91)90099-K.

Buccelletti, E., Gilardi, E., Scaini, E., Galiuto, L., Persiani, R., Biondi, a, Basile, F., Silveri, N.G., 2009. Heart rate variability and myocardial infarction: systematic literature review and metanalysis. Eur. Rev. Med. Pharmacol. Sci. 13, 299–307.

Bullmore, E., Sporns, O., 2009. Complex brain networks: graph theoretical analysis of structural and functional systems. Nat. Rev. Neurosci. 10 https://doi.org/10.1038/nrn2618, 312–312.

Cannon, W.B., 1929. Organization for physiological homeostasis. Physiol. Rev. 9, 399–431. https://doi.org/10.1152/physrev.1929.9.3.399.

Capuana, L.J., Dywan, J., Tays, W.J., Elmers, J.L., Witherspoon, R., Segalowitz, S.J., 2014. Factors influencing the role of cardiac autonomic regulation in the service of cognitive control. Biol. Psychol. 102, 88–97. https://doi.org/10.1016/j.biopsycho.2014.07.015.

Carnevali, L., Koenig, J., Sgoifo, A., Ottaviani, C., 2018. Autonomic and brain morphological predictors of stress resilience. Front. Neurosci. 12, 1–13. https://doi.org/10.3389/fnins.2018.00228.

Chang, C., Metzger, C.D., Glover, G.H., Duyn, J.H., Heinze, H.J., Walter, M., 2013. Association between heart rate variability and fluctuations in resting-state functional connectivity. Neuroimage 68, 93–104. https://doi.org/10.1016/j.neuroimage.2012.11.038.

Cox, R.W., 1996. AFNI: software for analysis and visualization of functional magnetic resonance neuroimages. Comput. Biomed. Res. 29, 162–173. https://doi.org/10.1006/cbmr.1996.0014.

Critchley, H.D., Corfield, D.R., Chandler, M.P., Mathias, C.J., Dolan, R.J., 2000. Cerebral correlates of autonomic cardiovascular arousal: a functional neuroimaging investigation in humans. J. Physiol. 523 (Pt 1), 259–270. https://doi.org/10.1111/j.1469-7793.2000.t01-1-00259.x.

Critchley, H.D., Mathias, C.J., Josephs, O., O'Doherty, J., Zanini, S., Dewar, B.K., Cipolotti, L., Shallice, T., Dolan, R.J., 2003. Human cingulate cortex and autonomic control: converging neuroimaging and clinical evidence. Brain 126, 2139–2152. https://doi.org/10.1093/brain/awg216.

Critchley, H.D., Nagai, Y., Gray, M.A., Mathias, C.J., 2011. Dissecting axes of autonomic control in humans: insights from neuroimaging. Auton. Neurosci. Basic Clin. 161, 34–42. https://doi.org/10.1016/j.autneu.2010.09.005.

Damoiseaux, J.S., Beckmann, C.F., Arigita, E.J.S., Barkhof, F., Scheltens, P., Stam, C.J., Smith, S.M., Rombouts, S.A.R.B., 2008. Reduced resting-state brain activity in the "default network" in normal aging. Cerebr. Cortex 18, 1856–1864. https://doi.org/10.1093/cercor/bhm207.

Damoiseaux, J.S., Rombouts, S.A.R.B., Barkhof, F., Scheltens, P., Stam, C.J., Smith, S.M., Beckmann, C.F., Raichle, M.E., 2006. Consistent Resting-state Networks across Healthy Subjects.

De Meersman, R.E., Stein, P.K., 2007. Vagal modulation and aging. Biol. Psychol. 74, 165–173. https://doi.org/10.1016/j.biopsycho.2006.04.008.

Demirtas-Tatlidede, A., Freitas, C., Pascual-Leone, A., Schmahmann, J.D., 2011. Modulatory effects of theta burst stimulation on cerebellar nonsomatic functions. Cerebellum 10, 495–503. https://doi.org/10.1007/s12311-010-0230-5.

Felber Dietrich, D., Schwartz, J., Schindler, C., Gaspoz, J.-M., Barthélémy, J.-C., Tschopp, J.-M., Roche, F., von Eckardstein, A., Brändli, O., Leuenberger, P.,

Gold, D.R., Ackermann-Liebrich, U., 2007. Effects of passive smoking on heart rate variability, heart rate and blood pressure: an observational study. Int. J. Epidemiol. 36, 834–840. https://doi.org/10.1093/ije/dym031.

Ferreira, L.K., Busatto, G.F., 2013. Resting-state functional connectivity in normal brain aging. Neurosci. Biobehav. Rev. 37, 384–400. https://doi.org/10.1016/j.neubiorev.2013.01.017.

Filippini, N., MacIntosh, B.J., Hough, M.G., Goodwin, G.M., Frisoni, G.B., Smith, S.M., Matthews, P.M., Beckmann, C.F., Mackay, C.E., 2009. Distinct patterns of brain activity in young carriers of the APOE- 4 allele. Proc. Natl. Acad. Sci. Unit. States Am. 106, 7209–7214. https://doi.org/10.1073/pnas.0811879106.

Fischl, B., 2012. FreeSurfer. Neuroimage 62, 774–781. https://doi.org/10.1016/j.neuroimage.2012.01.021.

Friston, K.J., Williams, S., Howard, R., Frackowiak, R.S.J., Turner, R., 1996. Movement-related effects in fMRI time-series. Magn. Reson. Med. 35, 346–355. https://doi.org/10.1002/mrm.1910350312.

García-García, I., Jurado, M.Á., Garolera, M., Marqués-Iturria, I., Horstmann, A., Segura, B., Pueyo, R., Sender-Palacios, M.J., Vernet-Vernet, M., Villringer, A., Junqué, C., Margulies, D.S., Neumann, J., 2015. Functional network centrality in obesity: a resting-state and task fMRI study. Psychiatry Res. Neuroimaging. 233, 331–338. https://doi.org/10.1016/j.pscychresns.2015.05.017.

Ghelarducci, B., Sebastiani, L., 1996. Contribution of the cerebellar vermis to cardiovascular control. J. Auton. Nerv. Syst. 56, 149–156. https://doi.org/10.1016/0165-1838(95)00068-2.

Gianaros, P.J., Van Der Veen, F., Jennings, J.R., 2004. Regional cerebral blood flow correlates with heart period and high-frequency heart period variability during working-memory task: implications for the cortical and subcortical regulation of cardiac autonomic activity. Psychophysiology 41, 521–530. https://doi.org/10.1111/j.1469-8986.2004.00179.x.

Gorgolewski, K., Burns, C.D., Madison, C., Clark, D., Halchenko, Y.O., Waskom, M.L., Ghosh, S.S., 2011. Nipype: a flexible, lightweight and extensible neuroimaging data processing framework in Python. Front. Neuroinf. 5, 13. https://doi.org/10.3389/fninf.2011.00013.

Gorgolewski, K.J., Varoquaux, G., Rivera, G., Schwarz, Y., Ghosh, S.S., Maumet, C., Sochat, V.V., Nichols, T.E., Poldrack, R.A., Poline, J.-B., Yarkoni, T., Margulies, D.S., 2015. NeuroVault.org: a web-based repository for collecting and sharing unthresholded statistical maps of the human brain. Front. Neuroinf. 9 https://doi.org/10.3389/fninf.2015.00008.

Gould van Praag, C.D., Garfinkel, S.N., Sparasci, O., Mees, A., Philippides, A.O., Ware, M., Ottaviani, C., Critchley, H.D., 2017. Mind-wandering and alterations to default mode network connectivity when listening to naturalistic versus artificial sounds. Sci. Rep. 7, 45273. https://doi.org/10.1038/srep45273.

Grady, C., 2012. The cognitive neuroscience of ageing. Nat. Rev. Neurosci. 13, 491–505. https://doi.org/10.1038/nrn3256.

Greenwood, P.M., 2007. Functional plasticity in cognitive aging: review and hypothesis. Neuropsychology 21, 657–673. https://doi.org/10.1037/0894-4105.21.6.657.

Greicius, M.D., Krasnow, B., Reiss, A.L., Menon, V., 2003. Functional connectivity in the resting brain: a network analysis of the default mode hypothesis. Proc. Natl. Acad. Sci. Unit. States Am. 100, 253–258. https://doi.org/10.1073/pnas.0135058100.

Griswold, M.A., Jakob, P.M., Heidemann, R.M., Nittka, M., Jellus, V., Wang, J., Kiefer, B., Haase, A., 2002. Generalized autocalibrating partially parallel acquisitions (GRAPPA). Magn. Reson. Med. 47, 1202–1210. https://doi.org/10.1002/mrm.10171.

Gusnard, D.A., Akbudak, E., Shulman, G.L., Raichle, M.E., 2001. Medial prefrontal cortex and self-referential mental activity: relation to a default mode of brain function. Proc. Natl. Acad. Sci. Unit. States Am. 98, 4259–4264. https://doi.org/10.1073/pnas.071043098.

Guterstam, A., Björnsdotter, M., Gentile, G., Ehrsson, H.H., 2015. Posterior cingulate cortex integrates the senses of self-location and body ownership. Curr. Biol. 25, 1416–1425. https://doi.org/10.1016/j.cub.2015.03.059.

Hagemann, D., Waldstein, S.R., Thayer, J.F., 2003. Central and autonomic nervous system integration in emotion. Brain Cognit. 52, 79–87. https://doi.org/10.1016/S0278-2626(03)00011-3.

Hansen, A.L., Johnsen, B.H., Sollers, J.J., Stenvik, K., Thayer, J.F., 2004. Heart rate variability and its relation to prefrontal cognitive function: the effects of training and detraining. Eur. J. Appl. Physiol. 93, 263–272. https://doi.org/10.1007/s00421-004-1208-0.

Hayano, J., Yamada, M., Sakakibara, Y., Fujinami, T., Yokoyama, K., Watanabe, Y., Takata, K., 1990. Short- and long-term effects of cigarette smoking on heart rate variability. Am. J. Cardiol. 65, 84–88. https://doi.org/10.1016/0002-9149(90)90030-5.

Hobert, M.A., Niebler, R., Meyer, S.I., Brockmann, K., Becker, C., Huber, H., Gaenslen, A., Godau, J., Eschweiler, G.W., Berg, D., Maetzler, W., 2011. Poor trail making test performance is directly associated with altered dual task prioritization in the elderly - baseline results from the trend study. PloS One 6. https://doi.org/10.1371/journal.pone.0027831.

Holzman, J.B., Bridgett, D.J., 2017. Heart rate variability indices as bio-markers of top-down self-regulatory mechanisms: a meta-analytic review. Neurosci. Biobehav. Rev. 74, 233–255. https://doi.org/10.1016/j.neubiorev.2016.12.032.

Huxley, R., Mendis, S., Zheleznyakov, E., Reddy, S., Chan, J., 2010. Body mass index, waist circumference and waist:hip ratio as predictors of cardiovascular riska review of the literature. Eur. J. Clin. Nutr. 64, 16–22. https://doi.org/10.1038/ejcn.2009.68.

Janssen, I., Katzmarzyk, P.T., Ross, R., 2002. Body mass index, waist circumference, and health risk. Arch. Intern. Med. 162, 2074. https://doi.org/10.1001/archinte.162.18.2074.

Jenkinson, M., Beckmann, C.F., Behrens, T.E.J., Woolrich, M.W., Smith, S.M., 2012. Fsl. Neuroimage 62, 782–790. https://doi.org/10.1016/j.neuroimage.2011.09.015.

Jennings, J.R., Sheu, L.K., Kuan, D.C.H., Manuck, S.B., Gianaros, P.J., 2016. Resting state connectivity of the medial prefrontal cortex covaries with individual differences in high-frequency heart rate variability. Psychophysiology 53, 444–454. https://doi.org/10.1111/psyp.12586.

Kanekiyo, T., Xu, H., Bu, G., 2014. ApoE and Aβ in Alzheimer's disease: accidental encounters or partners? Neuron. https://doi.org/10.1016/j.neuron.2014.01.045.

Kemp, A.H., Koenig, J., Thayer, J.F., 2017. From psychological moments to mortality: a multidisciplinary synthesis on heart rate variability spanning the continuum of time. Neurosci. Biobehav. Rev. https://doi.org/10.1016/j.neubiorev.2017.09.006.

Kemp, A.H., Quintana, D.S., 2013. The relationship between mental and physical health: insights from the study of heart rate variability. Int. J. Psychophysiol. 89, 288–296. https://doi.org/10.1016/j.ijpsycho.2013.06.018.

Kim, D.H., Lipsitz, L.A., Ferrucci, L., Varadhan, R., Guralnik, J.M., Carlson, M.C., Fleisher, L.A., Fried, L.P., Chaves, P.H.M., 2006. Association between reduced heart rate variability and cognitive impairment in older disabled women in the community: women's Health and Aging Study I. J. Am. Geriatr. Soc. 54, 1751–1757. https://doi.org/10.1111/j.1532-5415.2006.00940.x.

Koelsch, S., Skouras, S., Jentschke, S., 2013. Neural correlates of emotional personality: a structural and functional magnetic resonance imaging study. PloS One 8, e77196. https://doi.org/10.1371/journal.pone.0077196.

Koenig, J., Thayer, J.F., 2016. Sex differences in healthy human heart rate variability: a meta-analysis. Neurosci. Biobehav. Rev. 64, 288–310. https://doi.org/10.1016/j.neubiorev.2016.03.007.

Leaton, R., 2003. Fear and the cerebellum. Mol. Psychiatr. 8, 461–462. https://doi.org/10.1038/sj.mp.4001286.

Liao, D., Cai, J., Rosamond, W., Barnes, R., Hutchinson, R., Whitsel, E., Rautaharju, P., Heiss, G., 1997. Cardiac autonomic function and incident coronary heart disease: a population-based case-cohort study the ARIC study. Am. Jails 145, 696–706. https://doi.org/10.1093/aje/145.8.696.

Lipsitz, L.A., Goldberger, A.L., 1992. Loss of 'complexity' and aging: potential applications of fractals and chaos theory to senescence. JAMA, J. Am. Med. Assoc. 267, 1806–1809. https://doi.org/10.1001/jama.1992.03480130122036.

Loeffler, M., Engel, C., Ahnert, P., Alfermann, D., Arelin, K., Baber, R., Beutner, F., Binder, H., Brähler, E., Burkhardt, R., Ceglarek, U., Enzenbach, C., Fuchs, M., Glaesmer, H., Girlich, F., Hagendorff, A., Häntzsch, M., Hegerl, U., Henger, S., Hensch, T., Hinz, A., Holzendorf, V., Husser, D., Kersting, A., Kiel, A., Kirsten, T., Kratzsch, J., Krohn, K., Luck, T., Melzer, S., Netto, J., Nüchter, M., Raschpichler, M., Rauscher, F.G., Riedel-Heller, S.G., Sander, C., Scholz, M., Schönknecht, P., Schroeter, M.L., Simon, J.-C., Speer, R., Stäker, J., Stein, R., Stöbel-Richter, Y., Stumvoll, M., Tarnok, A., Teren, A., Teupser, D., Then, F.S., Tönjes, A., Treudler, R., Villringer, A., Weissgerber, A., Wiedemann, P., Zachariae, S., Wirkner, K., Thiery, J., 2015. The LIFE-Adult-Study: objectives and design of a population-based cohort study with 10,000 deeply phenotyped adults in Germany. BMC Publ. Health 15, 691. https://doi.org/10.1186/s12889-015-1983-z.

Lohmann, G., Margulies, D.S., Horstmann, A., Pleger, B., Lepsien, J., Goldhahn, D., Schloegl, H., Stumvoll, M., Villringer, A., Turner, R., 2010. Eigenvector centrality mapping for analyzing connectivity patterns in fMRI data of the human brain. PloS One 5, e10232. https://doi.org/10.1371/journal.pone.0010232.

Long, X., Benischek, A., Dewey, D., Lebel, C., 2017. Age-related functional brain changes in young children. Neuroimage 155, 322–330. https://doi.org/10.1016/j.neuroimage.2017.04.059.

Mahinrad, S., Jukema, J.W., Van Heemst, D., MacFarlane, P.W., Clark, E.N., De Craen, A.J.M., Sabayan, B., 2016. 10-Second heart rate variability and cognitive function in old age. Neurology 86, 1120–1127. https://doi.org/10.1212/WNL.0000000000002499.

Maier, S.U., Hare, T.A., 2017. Higher heart-rate variability is associated with ventromedial prefrontal cortex activity and increased resistance to temptation in dietary self-control challenges. J. Neurosci. 37, 446–455. https://doi.org/10.1523/JNEUROSCI.2815-16.2017.

Makovac, E., Garfinkel, S., Bassi, A., Basile, B., Macaluso, E., Cercignani, M., Calcagnini, G., Mattei, E., Mancini, M., Agalliu, D., Cortelli, P., Caltagirone, C., Critchley, H., Bozzali, M., 2017. Fear processing is differentially affected by lateralized stimulation of carotid baroreceptors. Cortex 99, 200–212. https://doi.org/10.1016/j.cortex.2017.07.002.

Margulies, D.S., Böttger, J., Long, X., Lv, Y., Kelly, C., Schäfer, A., Goldhahn, D., Abbushi, A., Milham, M.P., Lohmann, G., Villringer, A., 2010. Resting developments: a review of fMRI post-processing methodologies for spontaneous brain activity. Magn. Reson. Mater. Physics, Biol. Med. 23, 289–307. https://doi.org/10.1007/s10334-010-0228-5.

Marques, J.P., Kober, T., Krueger, G., van der Zwaag, W., Van de Moortele, P.F., Gruetter, R., 2010. MP2RAGE, a self bias-field corrected sequence for improved segmentation and T1-mapping at high field. Neuroimage 49, 1271–1281. https://doi.org/10.1016/j.neuroimage.2009.10.002.

Mather, M., Thayer, J.F., 2018. How heart rate variability affects emotion regulation brain networks. Curr. Opin. Behav. Sci. 19, 98–104. https://doi.org/10.1016/j.cobeha.2017.12.017.

McEwen, B.S., 2003. Interacting mediators of allostasis and allostatic load: towards an understanding of resilience in aging. Metabolism 52, 10–16. https://doi.org/10.1016/S0026-0495(03)00295-6.

Mennes, M., Zuo, X.N., Kelly, C., Di Martino, A., Zang, Y.F., Biswal, B., Castellanos, F.X., Milham, M.P., 2011. Linking inter-individual differences in neural activation and behavior to intrinsic brain dynamics. Neuroimage 54, 2950–2959. https://doi.org/10.1016/j.neuroimage.2010.10.046.

Molfino, A., Fiorentini, A., Tubani, L., Martuscelli, M., Fanelli, F.R., Laviano, A., 2009. Body mass index is related to autonomic nervous system activity as measured by

heart rate variability. Eur. J. Clin. Nutr. 63, 1263–1265. https://doi.org/10.1038/ejcn.2009.35.
Mueller, K., Arelin, K., Möller, H.E., Sacher, J., Kratzsch, J., Luck, T., Riedel-Heller, S., Villringer, A., Schroeter, M.L., 2016. Serum BDNF correlates with connectivity in the (pre)motor hub in the aging human brain-a resting-state fMRI pilot study. Neurobiol. Aging 38, 181–187. https://doi.org/10.1016/j.neurobiolaging.2015.11.003.
Munoz, M.L., Van Roon, A., Riese, H., Thio, C., Oostenbroek, E., Westrik, I., De Geus, E.J.C., Gansevoort, R., Lefrandt, J., Nolte, I.M., Snieder, H., 2015. Validity of (Ultra-)Short recordings for heart rate variability measurements. PloS One 10, 1–15. https://doi.org/10.1371/journal.pone.0138921.
Nussinovitch, U., Elishkevitz, K.P., Kaminer, K., Nussinovitch, M., Segev, S., Volovitz, B., Nussinovitch, N., 2011a. The efficiency of 10-second resting heart rate for the evaluation of short-term heart rate variability indices. PACE - Pacing Clin. Electrophysiol. 34, 1498–1502. https://doi.org/10.1111/j.1540-8159.2011.03178.x.
Nussinovitch, U., Elishkevitz, K.P., Katz, K., Nussinovitch, M., Segev, S., Volovitz, B., Nussinovitch, N., 2011b. Reliability of ultra-short ECG indices for heart rate variability. Ann. Noninvasive Electrocardiol. 16, 117–122. https://doi.org/10.1111/j.1542-474X.2011.00417.x.
Park, H.-D., Correia, S., Ducorps, A., Tallon-Baudry, C., 2014. Spontaneous fluctuations in neural responses to heartbeats predict visual detection. Nat. Neurosci. 17, 612–618. https://doi.org/10.1038/nn.3671.
Posner, J., Cha, J., Wang, Z., Talati, A., Warner, V., Gerber, A., Peterson, B.S., Weissman, M., 2016. Increased default mode network connectivity in individuals at high familial risk for depression. Neuropsychopharmacology 41, 1759–1767. https://doi.org/10.1038/npp.2015.342.
Power, J.D., Barnes, K.A., Snyder, A.Z., Schlaggar, B.L., Petersen, S.E., 2012. Spurious but systematic correlations in functional connectivity MRI networks arise from subject motion. Neuroimage 59, 2142–2154. https://doi.org/10.1016/j.neuroimage.2011.10.018.
Power, J.D., Schlaggar, B.L., Petersen, S.E., 2015. Recent progress and outstanding issues in motion correction in resting state fMRI. Neuroimage 105, 536–551. https://doi.org/10.1016/j.neuroimage.2014.10.044.
Price, J.L., 2007. Definition of the orbital cortex in relation to specific connections with limbic and visceral structures and other cortical regions. In: Annals of the New York Academy of Sciences, pp. 54–71. https://doi.org/10.1196/annals.1401.008.
Price, J.L., 1999. Prefrontal cortical networks related to visceral function and mood. In: Annals of the New York Academy of Sciences, pp. 383–396. https://doi.org/10.1111/j.1749-6632.1999.tb09278.x.
Raichle, M.E., MacLeod, A.M., Snyder, A.Z., Powers, W.J., Gusnard, D.A., Shulman, G.L., 2001. A default mode of brain function. Proc. Natl. Acad. Sci. Unit. States Am. 98, 676–682. https://doi.org/10.1073/pnas.98.2.676.
R Core Team, 2016. R: A Language and Environment for Statistical Computing. R Foundation for Statistical Computing, Vienna, Austria.
Reitan, R.M., 1955. Certain differential effects of left and right cerebral lesions in human adults. J. Comp. Physiol. Psychol. 48, 474–477.
Reitan, R.M., Wolfson, D., 1995. Category test and trail making test as measures of frontal lobe functions. Clin. Neuropsychol. 9, 50–56. https://doi.org/10.1080/13854049508402057.
Rokem, a, Trumpis, M., Perez, F., 2009. Nitime: time-series analysis for neuroimaging data. In: Proc. 8th Python Sci. Conf. (SciPy 2009) 1–8.
Rubinov, M., Sporns, O., 2010. Complex network measures of brain connectivity: uses and interpretations. Neuroimage 52, 1059–1069. https://doi.org/10.1016/j.neuroimage.2009.10.003.
Sacchetti, B., Baldi, E., Lorenzini, C.A., Bucherelli, C., 2002. Cerebellar role in fear-conditioning consolidation. Proc. Natl. Acad. Sci. Unit. States Am. 99, 8406–8411. https://doi.org/10.1073/pnas.112660399.
Sakaki, M., Yoo, H.J., Nga, L., Lee, T.-H., Thayer, J.F., Mather, M., 2016. Heart rate variability is associated with amygdala functional connectivity with MPFC across younger and older adults. Neuroimage 139, 44–52. https://doi.org/10.1016/j.neuroimage.2016.05.076.
Shehzad, Z., Kelly, A.M.C., Reiss, P.T., Gee, D.G., Gotimer, K., Uddin, L.Q., Lee, S.H., Margulies, D.S., Roy, A.K., Biswal, B.B., Petkova, E., Castellanos, F.X., Milham, M.P., 2009. The resting brain: unconstrained yet reliable. Cerebr. Cortex 19, 2209–2229. https://doi.org/10.1093/cercor/bhn256.
Sin, N.L., Sloan, R.P., McKinley, P.S., Almeida, D.M., 2016. Linking daily stress processes and laboratory-based heart rate variability in a national sample of midlife and older adults. Psychosom. Med. 78, 573–582. https://doi.org/10.1097/PSY.0000000000000306.
Singh, J.P., Larson, M.G., Tsuji, H., Evans, J.C., O'Donnell, C.J., Levy, D., 1998. Reduced heart rate variability and new-onset hypertension: insights into pathogenesis of hypertension: the Framingham Heart Study. Hypertension 32, 293–297. https://doi.org/10.1161/01.HYP.32.2.293.
Smith, R., Thayer, J.F., Khalsa, S.S., Lane, R.D., 2017. The hierarchical basis of neurovisceral integration. Neurosci. Biobehav. Rev. 75, 274–296. https://doi.org/10.1016/j.neubiorev.2017.02.003.
Smith, S.M., Nichols, T.E., Vidaurre, D., Winkler, A.M., Behrens, T.E.J., Glasser, M.F., Ugurbil, K., Barch, D.M., Van Essen, D.C., Miller, K.L., 2015. A positive-negative mode of population covariation links brain connectivity, demographics and behavior. Nat. Neurosci. 18, 1565–1567. https://doi.org/10.1038/nn.4125.
Streitbürger, D.P., Pampel, A., Krueger, G., Lepsien, J., Schroeter, M.L., Mueller, K., Möller, H.E., 2014. Impact of image acquisition on voxel-based-morphometry investigations of age-related structural brain changes. Neuroimage 87, 170–182. https://doi.org/10.1016/j.neuroimage.2013.10.051.
Swank, A.M., 1996. Physical dimensions of aging. Med. Sci. Sports Exerc. 28, 398–399. https://doi.org/10.1097/00005768-199603000-00018.
Tarvainen, M.P., Niskanen, J.-P., Lipponen, J.A., Ranta-Aho, P.O., Karjalainen, P.A., 2014. Kubios HRV–heart rate variability analysis software. Comput. Methods Progr. Biomed. 113, 210–220. https://doi.org/10.1016/j.cmpb.2013.07.024.
Task Force of the European Society of Cardiology and the North American Society of Pacing and Electrophysiology, 1996. Heart rate variability: Standards of measurement, physiological interpretation, and clinical use. Circulation 93, 1043–1065.
Tataranni, P.A., Gautier, J.F., Chen, K., Uecker, A., Bandy, D., Salbe, A.D., Pratley, R.E., Lawson, M., Reiman, E.M., Ravussin, E., 1999. Neuroanatomical correlates of hunger and satiation in humans using positron emission tomography. Proc. Natl. Acad. Sci. U. S. A 96, 4569–4574. https://doi.org/10.1073/pnas.96.8.4569.
Taubert, M., Lohmann, G., Margulies, D.S., Villringer, A., Ragert, P., 2011. Long-term effects of motor training on resting-state networks and underlying brain structure. Neuroimage 57, 1492–1498. https://doi.org/10.1016/j.neuroimage.2011.05.078.
Thayer, J.F., Åhs, F., Fredrikson, M., Sollers, J.J., Wager, T.D., 2012. A meta-analysis of heart rate variability and neuroimaging studies: implications for heart rate variability as a marker of stress and health. Neurosci. Biobehav. Rev. 36, 747–756. https://doi.org/10.1016/j.neubiorev.2011.11.009.
Thayer, J.F., Lane, R.D., 2007. The role of vagal function in the risk for cardiovascular disease and mortality. Biol. Psychol. 74, 224–242. https://doi.org/10.1016/j.biopsycho.2005.11.013.
Thayer, J.F., Lane, R.D., 2000. A model of neurovisceral integration in emotion regulation and dysregulation. J. Affect. Disord. 61, 201–216. https://doi.org/10.1016/S0165-0327(00)00338-4.
Thayer, J.F., Ruiz-Padial, E., 2006. Neurovisceral integration, emotions and health: an update. Int. Congr. Ser. 1287, 122–127. https://doi.org/10.1016/j.ics.2005.12.018.
Thayer, J.F., Sollers, J.J., Friedman, B.H., Koenig, J., 2015. Gender differences in the relationship between resting heart rate variability and 24-hour blood pressure variability. Blood Press. 7051, 1–5. https://doi.org/10.3109/08037051.2016.1090721.
Thayer, J.F., Sollers, J.J., Labiner, D.M., Weinand, M., Herring, A.M., Lane, R.D., Ahern, G.L., 2009. Age-related differences in prefrontal control of heart rate in humans: a pharmacological blockade study. Int. J. Psychophysiol. 72, 81–88. https://doi.org/10.1016/j.ijpsycho.2008.04.007.
Thayer, J.F., Yamamoto, S.S., Brosschot, J.F., 2010. The relationship of autonomic imbalance, heart rate variability and cardiovascular disease risk factors. Int. J. Cardiol. 141, 122–131. https://doi.org/10.1016/j.ijcard.2009.09.543.
Then, F.S., Luck, T., Luppa, M., Arélin, K., Schroeter, M.L., Engel, C., Löffler, M., Thiery, J., Villringer, A., Riedel-Heller, S.G., 2014. Association between mental demands at work and cognitive functioning in the general population – results of the health study of the Leipzig research center for civilization diseases (LIFE). J. Occup. Med. Toxicol. 9, 23. https://doi.org/10.1186/1745-6673-9-23.
Tombaugh, T.N., 2004. Trail Making Test A and B: normative data stratified by age and education. Arch. Clin. Neuropsychol. 19, 203–214. https://doi.org/10.1016/S0887-6177(03)00039-8.
Tukey, J.W., 1977. Exploratory Data Analysis. Addison-Wesley, Reading, MA.
Uddin, L.Q., Kelly, A.M.C., Biswal, B.B., Castellanos, F.X., Milham, M.P., 2009. Functional connectivity of default mode network components: correlation, anticorrelation, and causality. Hum. Brain Mapp. 30, 625–637. https://doi.org/10.1002/hbm.20531.
Umetani, K., Singer, D.H., McCraty, R., Atkinson, M., 1998. Twenty-four hour time domain heart rate variability and heart rate: relations to age and gender over nine decades. J. Am. Coll. Cardiol. 31, 593–601. https://doi.org/10.1016/S0735-1097(97)00554-8.
Van Eden, C.G., Buijs, R.M., 2000. Functional neuroanatomy of the prefrontal cortex: autonomic interactions. Prog. Brain Res. 126, 49–62. https://doi.org/10.1016/S0079-6123(00)26006-8.
Voss, A., Schroeder, R., Heitmann, A., Peters, A., Perz, S., 2015. Short-term heart rate variability - influence of gender and age in healthy subjects. PloS One 10, e0118308. https://doi.org/10.1371/journal.pone.0118308.
Wei, L., Chen, H., Wu, G.R., 2018. Heart rate variability associated with grey matter volumes in striatal and limbic structures of the central autonomic network. Brain Res. 1681, 14–20. https://doi.org/10.1016/j.brainres.2017.12.024.
Williams, D.P., Cash, C., Rankin, C., Bernardi, A., Koenig, J., Thayer, J.F., 2015. Resting heart rate variability predicts self-reported difficulties in emotion regulation: a focus on different facets of emotion regulation. Front. Psychol. 6, 1–8. https://doi.org/10.3389/fpsyg.2015.00261.
Wink, A.M., de Munck, J.C., van der Werf, Y.D., van den Heuvel, O.A., Barkhof, F., 2012. Fast eigenvector centrality mapping of voxel-wise connectivity in functional magnetic resonance imaging: implementation, validation, and interpretation. Brain Connect. 2, 265–274. https://doi.org/10.1089/brain.2012.0087.
Winkelmann, T., Thayer, J.F., Pohlack, S., Nees, F., Grimm, O., Flor, H., 2017. Structural brain correlates of heart rate variability in a healthy young adult population. Brain Struct. Funct. 222, 1061–1068. https://doi.org/10.1007/s00429-016-1185-1.
Wong, S.W., Massé, N., Kimmerly, D.S., Menon, R.S., Shoemaker, J.K., 2007. Ventral medial prefrontal cortex and cardiovagal control in conscious humans. Neuroimage 35, 698–708. https://doi.org/10.1016/j.neuroimage.2006.12.027.
Yoo, H.J., Thayer, J.F., Greening, S., Lee, T.-H., Ponzio, A., Min, J., Sakaki, M., Nga, L., Mather, M., Koenig, J., 2017. Brain structural concomitants of resting state heart rate variability in the young and old: evidence from two independent samples. Brain Struct. Funct. https://doi.org/10.1007/s00429-017-1519-7.
Yu, C., Zhou, Y., Liu, Y., Jiang, T., Dong, H., Zhang, Y., Walter, M., 2011. Functional segregation of the human cingulate cortex is confirmed by functional connectivity based neuroanatomical parcellation. Neuroimage 54, 2571–2581. https://doi.org/10.1016/j.neuroimage.2010.11.018.
Zeki Al Hazzouri, A., Haan, M.N., Deng, Y., Neuhaus, J., Yaffe, K., 2014. Reduced heart rate variability is associated with worse cognitive performance in elderly

Mexican Americans. Hypertension 63, 181–187. https://doi.org/10.1161/Hypertensionaha.113.01888.

Zulfiqar, U., Jurivich, D.A., Gao, W., Singer, D.H., 2010. Relation of high heart rate variability to healthy longevity. Am. J. Cardiol. 105, 1181–1185. https://doi.org/10.1016/j.amjcard.2009.12.022.

Zuo, X.-N., Di Martino, A., Kelly, C., Shehzad, Z.E., Gee, D.G., Klein, D.F., Castellanos, F.X., Biswal, B.B., Milham, M.P., 2010. The oscillating brain: complex and reliable. Neuroimage 49, 1432–1445. https://doi.org/10.1016/J.Neuroimage.2009.09.037.

Zuo, X.N., Ehmke, R., Mennes, M., Imperati, D., Castellanos, F.X., Sporns, O., Milham, M.P., 2012. Network centrality in the human functional connectome. Cerebr. Cortex 22, 1862–1875. https://doi.org/10.1093/cercor/bhr269.